Thermodynamic Properties of Refrigerant R116 from Cubic Equations of State

DANIELA DUNA, MIRELA IONITA, VIOREL FEROIU*, DAN GEANA
Politehnica University Bucharest, Department of Applied Physical Chemistry and Electrochemistry, 1 Polizu Str., 011061, Bucharest, Romania

Thermodynamic properties were predicted, for saturated phases and in the single-phase region for refrigerant R116 (C_2F_6). Five cubic equations of state were used: Soave-Redlich-Kwong (SRK), Peng-Robinson (PR), Schmidt-Wenzel (SW), Trebble-Bishnoi-Salim (TBS) and GEOS3C. A wide comparison with recommended NIST (National Institute of Standard and Technology, USA) data, considered as pseudo-experimental data was made. This study shows that the cubic EOSs lead to reasonable predictions of thermodynamic properties of refrigerant R116, resting simple enough for applications.

Keywords: *equation of state, vapor - liquid equilibrium, thermodynamic properties, refrigerants*

Refrigerants are the working fluids in refrigeration, air-conditioning and heat pumping systems. The Montreal protocol, in 1987, has prohibited the use and the production of chlorofluorocarbons (CFC's) in industrialized countries. Accurate thermodynamic properties of mixtures containing hydrofluorocarbons (HFC's), which are used as alternative refrigerants, are of great importance to design the refrigeration cycles and to determine the optimum new working fluids.

The practical importance of HFC's has determined numerous experimental studies. The significant amount of experimental data on these compounds has allowed derivation of accurate empirical models for interpolating their thermodynamic properties. However the development of models for prediction of phase equilibria and thermodynamic properties, as well as the improvement of modern equations of state (EOSs), are research themes of interest for the applications of refrigerants [1-4].

The hexafluoroethane (R116), is an environmentally acceptable refrigerant (the ozone depletion potential is zero) and presents interest in the search for alternative refrigerants. In our previous works [5-7] pure refrigerant properties were calculated by cubic equations of state. The purpose of this work is to present the result of simultaneous vapor – liquid equilibrium, thermodynamic and volumetric properties prediction of R116 pure fluid, and to compare the results with recommended NIST (National Institute of Standard and Technology, USA) data [8], considered as pseudo-experimental data. Five cubic equations of state were used: Soave-Redlich-Kwong (SRK) [9], Peng-Robinson (PR) [10], Schmidt-Wenzel (SW) [11], Trebble-Bishnoi-Salim (TBS) [12] and GEOS3C [13].

Recently, molecular theories have been implemented for the development of new thermodynamic models, such as Statistical Association Fluid Theory (SAFT) in equations of state. SAFT EOS models exhibit unrealistic and even nonphysical predictions due to the two factors: the temperature dependencies of a segment packing fraction and the high-polynomial orders by volume [14]. The first factor leads to nonphysical negative values of the heat capacities at very high pressures and the intersections of isotherms at high densities. The second factor is responsible for prediction of the additional unrealistic critical points and the fictive phase equilibria [14]. On the other hand, cubic equations of state exhibit an overall robustness in predicting various thermodynamic properties over a wide range of temperatures and pressures, with the exception of certain phenomena related to heat capacity, sound velocity and Joule-Thomson coefficient [5].

This study shows that the cubic EOSs lead to reasonable predictions of thermodynamic properties of R116, resting simple enough for applications in chemical engineering.

Regarding the terminology, it should be noted that the syntagma "thermodynamic properties" is used commonly in the chemical engineering literature, while "thermophysical properties" is used mainly in physics journals.

The GEOS3C equation of state

The GEOS3C equation of state is a general form [5, 6, 13] for the cubic equations of state with two, three and four parameters:

$$P = \frac{RT}{V-b} - \frac{a(T)}{(V-d)^2 + c} \tag{1}$$

The four parameters a, b, c, d for a pure component are expressed by:

$$a = a_c \beta^2(T_r); \quad a_c = \Omega_a \frac{R^2 T_c^2}{P_c}; \quad b = \Omega_b \frac{RT_c}{P_c};$$

$$c = \Omega_c \frac{R^2 T_c^2}{P_c^2}; \quad d = \Omega_d \frac{RT_c}{P_c}; \tag{2}$$

The GEOS3C equation uses the temperature function:

$$\beta(T_r) = 1 + C_1 y + C_2 y^2 + C_3 y^3 \qquad for\ T_r \le 1 \tag{3}$$

$$\beta(T_r) = 1 + C_1 y \qquad for\ T_r > 1 \tag{4}$$

$$y = 1 - \sqrt{T_r} \tag{5}$$

The expressions of the parameters Ω_a, Ω_b, Ω_c, Ω_d are:

* email: v_feroiu@chim.upb.ro; Tel: +4021 4023988

$$\Omega_a = (1-B)^3; \quad \Omega_b = Z_c - B;$$
$$\Omega_c = (1-B)^2(B-0.25); \quad \Omega_d = Z_c - 0.5(1-B) \tag{6}$$

$$B = \frac{1+C_1}{\alpha_c + C_1} \qquad \alpha_c \text{ - Riedel's criterion} \tag{7}$$

As pointed out previously [5], the relations (6) are general forms for all the cubic equations of state with two, three and four parameters. The calculated values Ω_a, Ω_b, W_c, Ω_d from equations (6) for all cubic EOSs are plotted in figure 1. The highest absolute values for Ω_a, Ω_b, Ω_d coefficients are those of GEOS. The SRK equation has the highest value for Ω_c coefficient. It must be mentioned that the parameters Ω_a, Ω_b, Ω_c, Ω_d for SRK and PR equations have unique values for all substances.

The software used in calculations is based on these equations for the reduction of GEOS to different cubic EOS from the literature. This is the meaning of the statement "general cubic equation of state" used for GEOS.

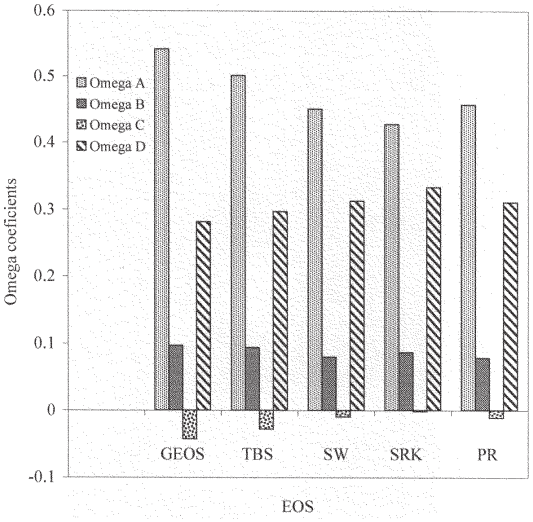

Fig. 1. Values of W_a, W_b, W_c, W_d for the cubic EOSs

The departure (residual) thermodynamic properties from the ideal gas at the same temperature and pressure are given for GEOS in a previous work [5]. The same relations were used for all EOSs under appropriate restrictions imposed for GEOS parameters. The ideal gas contribution to the thermodynamic properties was calculated using the heat capacity functions recommended in [15].

Results and discussions

In order to calculate the phase equilibrium and the thermodynamic properties for R116 the following equations of state have been used: Soave-Redlich-Kwong (SRK), Peng-Robinson (PR), Schmidt-Wenzel (SW), Trebble-Bishnoi-Salim (TBS) and GEOS3C. The investigated *PVT* range covers single-phase (liquid or gas) and two-phase (liquid-vapor) regions, using recommended NIST data as pseudo-experimental values. The calculations were made with the software package PHEQ (Phase Equilibria) developed in our laboratory [16].

Using NIST values of the critical constants and the acentric factor for the calculation of α_c from the equation:

$$\alpha_c = 5.808 + 4.93\omega \tag{8}$$

the C_1, C_2 and C_3 parameters were obtained by constraining the equation of state to reproduce the NIST vapor pressure data and liquid volumes on the saturation curve.

The values of C_1, C_2, C_3 parameters for the GEOS3C equation, the critical data and acentric factor for R116 are given in table 1.

The following thermodynamic properties have been predicted: compressibility factor (*Z*), enthalpy (*H*), enthalpy of vaporization ($\Delta^v H$), entropy (*S*), heat capacity at constant pressure (C_P), heat capacity at constant volume (C_V), heat capacity ratio (C_P/C_V), speed of sound (*Ws*), fugacity coefficient (φ), Joule-Thomson coefficient, (*JT*). No data on these thermodynamic properties were used in this work to obtain the GEOS parameters.

The results of the calculations for *PVT* and thermodynamic properties of R116 are summarized in tables 2-4.

In tables 2-4 the average absolute deviations (AAD), between calculated values by EOSs and NIST recommended data are reported. For each table the number of data points, the pressure and temperature ranges are indicated. The two-phase region properties have been calculated at temperatures from the triple point to the critical point.

The average absolute deviations for a property *Y* are relative (%):

$$\text{AAD \%} = \frac{\sum_{i=1}^{N} \left| (Y_i^{eos} - Y_i^{exp}) / Y_i^{exp} \right| \cdot 100}{N} \tag{9}$$

excepting the enthalpy and entropy where:

$$\text{AAD } H \text{ (or } S) = \frac{\sum_{i=1}^{N} \left| H_i^{eos} - H_i^{exp} \right|}{N} \tag{10}$$

As can be seen in tables 2-4, the vapour pressures and liquid saturated volumes are better reproduced by GEOS3C, compared to the results obtained using other equations. The liquid volumes calculated with the SRK and PR equations are in poor agreement with experimental data (9.5 and 6.2 % average deviation). The vapour volumes are well predicted by all equations of state.

All EOS's predict well the enthalpies and the entropies on the saturation curve, and also the heat capacities, the heat capacity ratio and the speed of sound in the same range. It can be remarked that the speed of sound deviations in liquid phase, predicted by TBS equation, are lower than those of other equations. The AAD% given in

Table 1
VALUES OF C_1, C_2, C_3 PARAMETERS FOR R116. CRITICAL DATA AND ACENTRIC FACTOR FROM NIST DATABASE [8]

Component	C_1	C_2	C_3	T_c (K)	P_c (bar)	Z_c	ω
R116	0.3784	0.3682	0.4252	293.03	30.48	0.2815	0.257

Table 2
PVT AND THERMODYNAMIC FUNCTION DEVIATIONS ON THE SATURATION CURVE FOR **R116**. TEMPERATURE RANGE (K):173.1 – 293.03. PRESSURE RANGE (BAR): 0.26 – 30.47 . NUMBER OF DATA POINTS: 62.

	AAD (%)				AAD			
EOS	P^S	V^L	V^V	$\Delta_{vap}H$	H^L (kJ/kg)	H^V (kJ/kg)	S^L (kJ/kg/K)	S^V (kJ/kg/K)
SRK	0.9	9.5	1.0	2.8	3.8	3.0	0.03	0.03
PR	0.4	6.2	1.2	2.2	2.6	2.6	0.03	0.03
SW	0.3	4.9	0.7	1.9	2.1	1.6	0.03	0.03
TBS	0.4	2.8	1.9	2.9	4.6	5.4	0.02	0.02
GEOS3C	0.2	2.2	2.7	3.8	4.0	5.3	0.02	0.02

table 3 for the JT coefficients in the saturated liquid range are relatively high, determined by very small values ($\sim 10^{-4}$) of the NIST JT coefficients at temperatures where the function changes the sign.

The difference in predictions between the EOSs is less noticeable for all thermodynamic properties in the single phase region excepting JT coefficient.

Representative examples of calculated properties in comparison with NIST data are provided in the figures 2-16. Figures 2 and 3 depict pressure – density diagrams for R116. Points figure NIST data, while the curves are calculated with the GEOS3C and SRK equations, for the saturation region and subcritical and supercritical isotherms. The liquid saturated densities calculated with the GEOS3C equation are in better agreement with the experimental data (NIST), in comparison with the densities calculated by the SRK equation. As pointed out already, liquid saturated densities have been used for the C_1, C_2 and C_3 parameter fitting of GEOS model. A similar fitting for SRK or PR equations does not improve the liquid densities, a translation in volume being necessary. For SW and TBS EOSs we used the generalization equations of their adjustable parameters.

The figures 4-5 show the deviations of vapour pressure and saturated liquid density, for the five EOSs in comparison

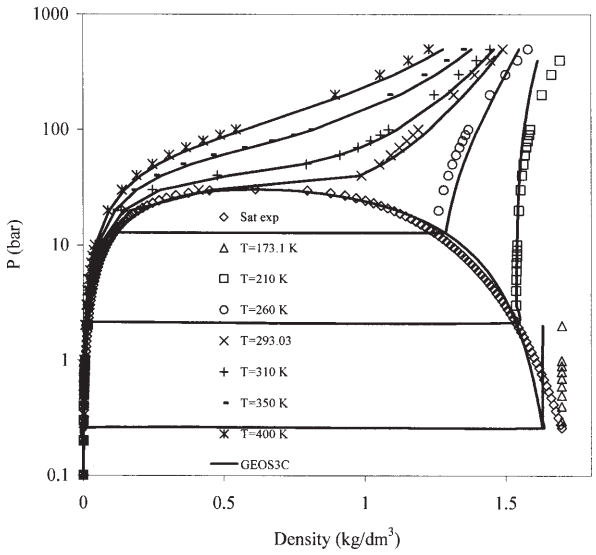

Fig. 2. Pressure–density diagram for R116. Points: NIST data [8]. Lines: prediction with the GEOS3C equation

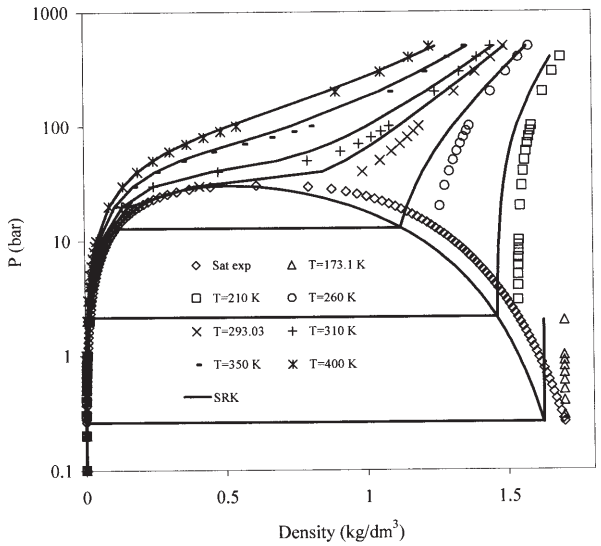

Fig. 3. Pressure–density diagram for R116. Points: NIST data [8]. Lines: prediction with the SRK equation

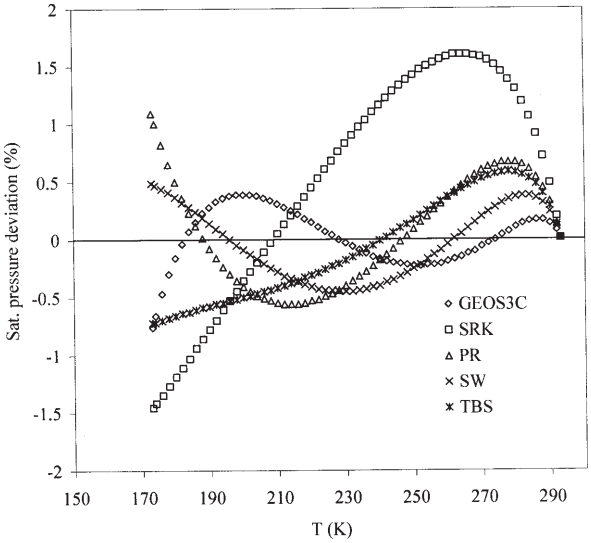

Fig. 4. Vapour pressure deviations relative to NIST data, obtained with cubic equations of state

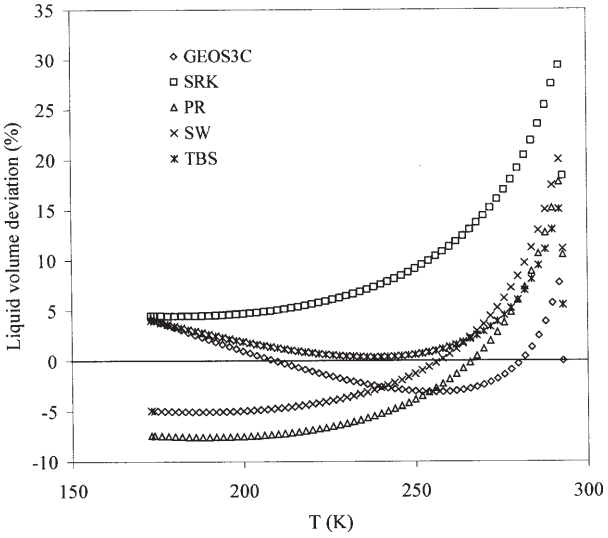

Fig. 5. Saturated liquid volume deviations relative to NIST data, obtained with cubic equations of state

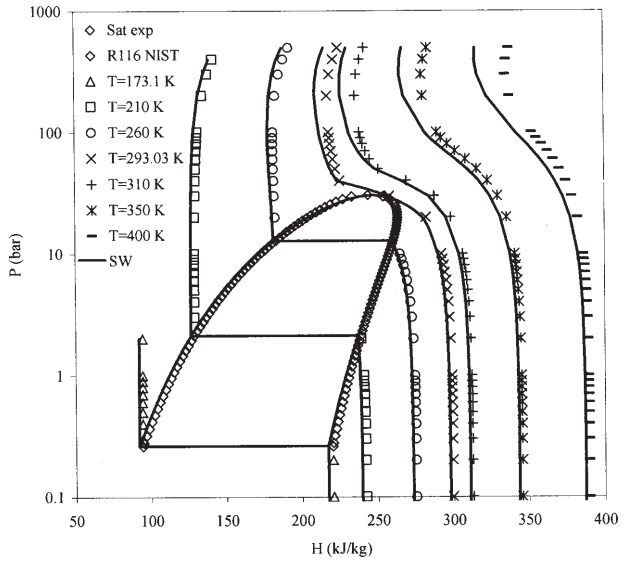

Fig.6. Pressure–enthalpy diagram for R116. Points: NIST data [8]. Lines: prediction with the SW equation

with NIST recommended data. The lowest deviations for both properties are given by GEOS3C equation.

The calculated enthalpies and entropies with SW and GEOS3C equations, on the saturation curve and in the single phase region, are depicted in figure 6 and figure 7 (points:

NIST recommended data). Both models under consideration yield comparable accuracy in predicting enthalpies and entropies.

The next property to be considered, the isochoric heat capacity of the saturated phases (fig. 8) is difficult for accurate prediction due to the inability of cubic equations of state to yield the infinite value of C_V at critical temperature. The isochoric heat capacity (C_V) predictions of saturated phases from GEOS3C, SRK, PR, TBS and SW equations are shown in the figure 8. As can be observed, the cubic EOSs predict a different pattern of this curve in comparison with NIST data. All models yield comparable predictions in isochoric heat capacities of the saturated vapors, but deteriorate for the saturated liquid and in the region approaching the critical point.

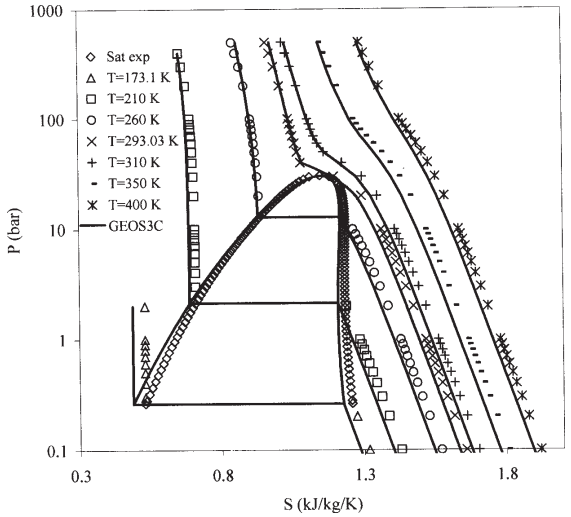

Fig. 7. Pressure–entropy diagram for R116. Points: NIST data [8]. Lines: prediction with the GEOS3C equation.

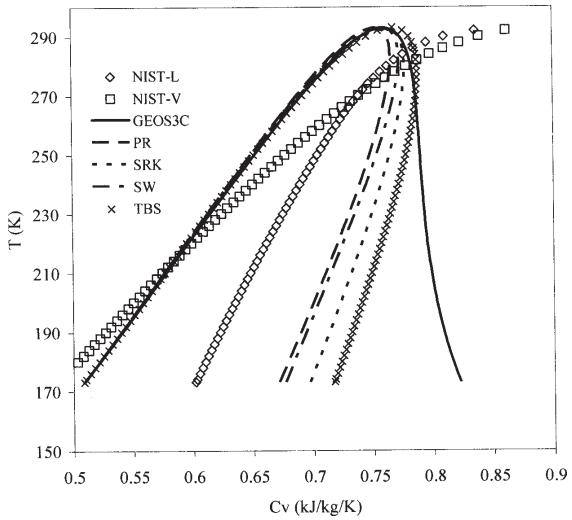

Fig.8. Temperature-isochoric heat capacity diagram (saturation curve) of R116. Points: NIST data [8]. Lines: prediction with the GEOS3C, TBS, SW, PR and SRK equations

The temperature-isobaric heat capacity diagram (saturation curve) of R116 is presented in figure 9. Points figure NIST data while the curves are calculated with the GEOS3C and PR equations. The values predicted by PR equation are in slightly better agreement with NIST data for the saturated liquid. Both models yield comparable predictions in isobaric heat capacities of the saturated vapours. The tendency to infinite value of C_p at the critical point is satisfactorily predicted by both equations.

The figure 10 shows the pressure – speed of sound diagram predicted by TBS equation for R116, in the entire

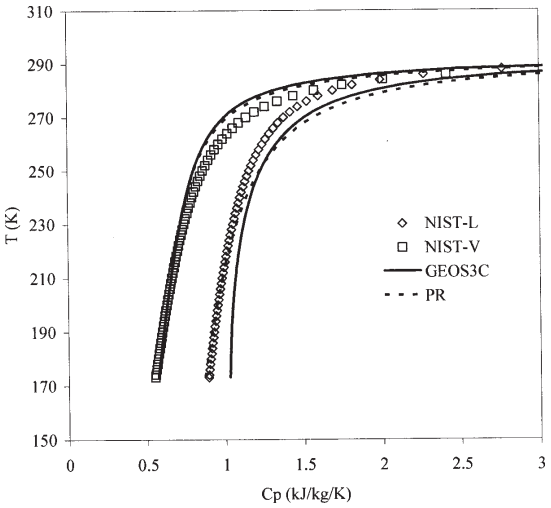

Fig.9. Temperature–isobaric heat capacity diagram (saturation curve) of R116. Points: NIST data [8]. Lines: prediction with the GEOS3C and PR equations.

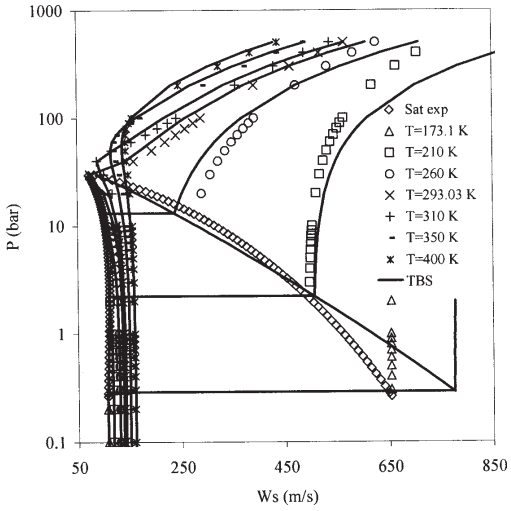

Fig. 10. Pressure–speed of sound diagram for R116. Points: NIST data [12]. Lines: prediction with the TBS equation

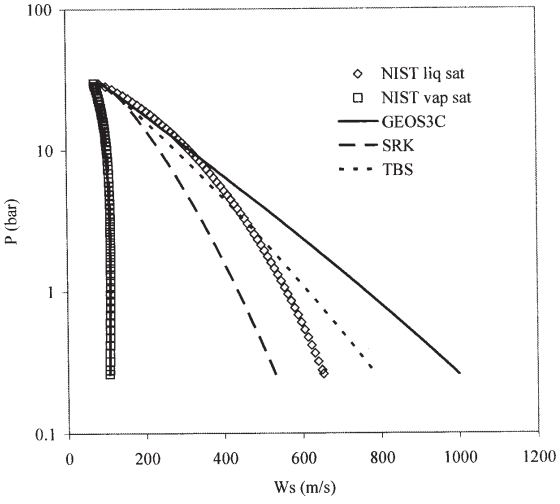

Fig. 11. Pressure–speed of sound dependence of saturated phases, for R116. Points: NIST data [8]. Lines: prediction with GEOS3C, TBS and SRK equations

range of T and P. The predicted values of this equation are in better agreement with the NIST data (tables 3-4). The pressure – speed of sound dependence of saturated phases is plotted in figure 11, for the GEOS3C, TBS and SRK equations. The models under consideration yield comparable accuracy in predicting speed of sound of the saturated vapours, but perform differently for the saturated

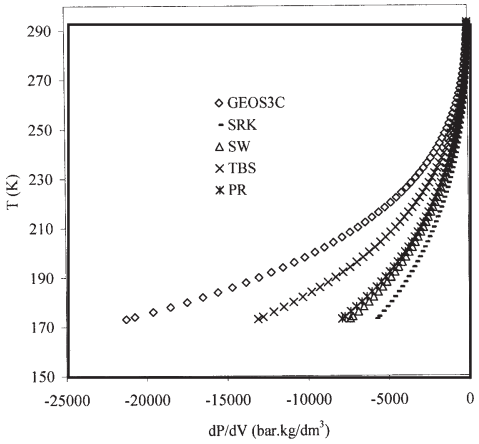

Fig. 12. Dependence of derivative $(\partial P / \partial V)_T$ of temperature, for the saturated liquid

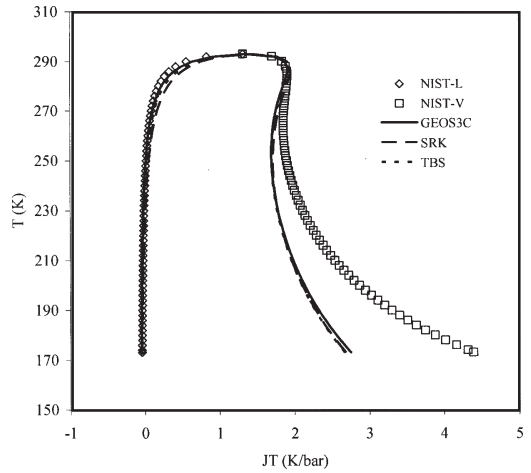

Fig. 13. Joule-Thomson coefficient prediction of saturated phases for R116 by GEOS3C, TBS and SRK equations. Points: NIST data [8]

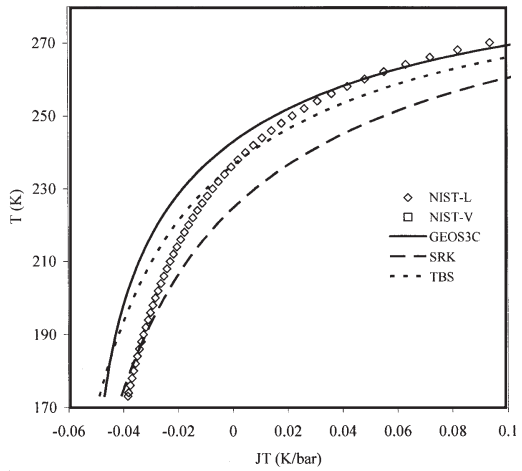

Fig. 14. Joule-Thomson coefficient prediction of liquid phase for R116 by GEOS3C, TBS and SRK equations. Points: NIST data [8]

liquid. The speed of sound is calculated from the following equation:

$$W_S = \left[-\frac{C_P}{C_V} \frac{V^2}{M} \left(\frac{\partial P}{\partial V} \right)_T \right]^{0,5} \quad (11)$$

As seen in table 3, the C_p/C_V ratio is reproduced with the same accuracy by all considered EOSs. In order to explain the different behaviour of the EOS's in figure 11, the dependence of derivative $(\partial P / \partial V)_T$ on temperature, of the saturated liquid, is shown for all EOSs in figure 12. As can be seen GEOS yields the highest negative value of this derivative in comparison to the other cubic EOSs. This

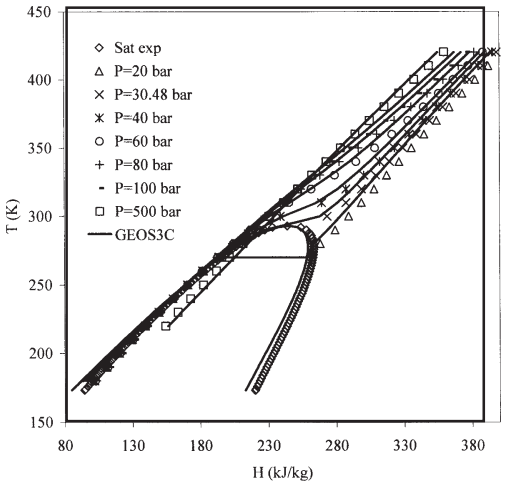

Fig. 15. Temperature–enthalpy diagram for R116 (saturation curve and isobars). Points: NIST data [8]. Lines: prediction with GEOS3C equation

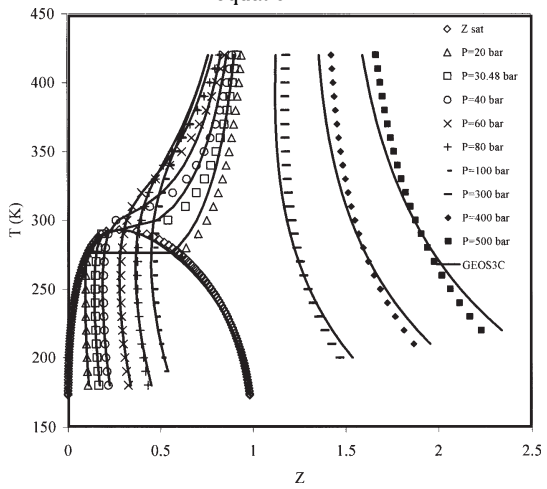

Fig. 16. Temperature-compressibility factor diagram for R116 (saturation curve and isobars). Points: NIST data [8]. Lines: prediction with GEOS3C equation.

behaviour explains the higher values of predicted speed of sound by GEOS equation in liquid phase as well as the lower values predicted by SRK equation (fig. 11). The positive deviations of GEOS and the negative deviations of SRK equation relative to NIST data lead to approximately equal AAD % of both equations in table 3. It results from this analysis that the good correlation of vapour pressure and saturated liquid density does not guarantee accurate values of the derivative $(\partial P / \partial V)_T$ of the saturated liquid.

Joule-Thomson coefficient predictions of the saturated phases for R116 by GEOS3C, TBS and SRK equations are depicted in figure13. The models under consideration yield apparently comparable accuracy in predicting Joule-Thomson coefficient of the saturated liquid, but deviate from NIST data for the saturated vapour. As seen in the figure 14, the predicted values are in better agreement with the NIST data for TBS equation in the liquid phase (see table 3 too).

In the NIST data base [8] there are available isobaric properties of pure fluids. It is of interest to see the quality of predictions of thermodynamic properties in isobaric conditions. The temperature–enthalpy and temperature–compressibility factor diagrams for R116 (saturated phases and isobars) predicted by GEOS3C equation are plotted in figure 15 and 16 (points represent NIST data). The predicted properties are of same accuracy as those obtained for isotherms. Moreover, the GEOS predictions reproduce the pattern of properties in isobaric diagrams, for example the

	AAD (%)							
EOS	C_P^L	C_P^V	$(C_P/C_V)^L$	$(C_P/C_V)^V$	W_S^L	W_S^V	JT^L	JT^V
SRK	9.8	4.9	11.5	1.8	21.1	0.5	191.7	16.5
PR	7.7	5.5	11.2	2.1	21.1	1.0	163.9	16.1
SW	8.5	5.3	11.5	2.1	20.9	0.7	168.1	16.0
TBS	8.8	5.9	10.4	2.9	9.4	1.8	33.5	16.2
GEOS3C	10.4	6.6	10.9	3.6	18.7	2.9	102.8	16.4

Table 3
THERMODYNAMIC FUNCTION DEVIATIONS AT SATURATION FOR **R116**. TEMPERATURE RANGE (K): 173.1 – 293.03. PRESSURE RANGE (MPa): (BAR): 0.26 – 30.47.NUMBER OF DATA POINTS: 62.

	AAD		AAD (%)				
EOS	S kJ/kg/K	H kJ/kg	Z	C_P	W_S	C_P/C_V	JT
SRK	0.02	3.9	1.5	1.7	4.4	2.3	19.6
PR	0.02	3.4	2.0	1.8	4.5	2.3	24.0
SW	0.03	3.2	1.5	2.4	4.5	2.5	30.9
TBS	0.02	5.7	1.1	2.3	3.3	2.7	18.3
GEOS3C	0.02	5.8	1.4	3.6	7.1	2.7	24.8

Table 4
THERMODYNAMIC FUNCTION DEVIATIONS IN SINGLE-PHASE REGION FOR **R116**. TEMPERATURE RANGE (K): 173.1 – 500. PRESSURE RANGE (BAR): 0.011–500. NUMBER OF DATA POINTS: 352

enthalpy and compressibility factor on isobars crossing the saturated range.

Conclusions

The vapour – liquid equilibrium and the thermodynamic properties of refrigerant R116 were predicted by five equations of state SRK, PR, SW, TBS and GEOS3C on a wide *PVT* range, including the entire saturation region. A large comparison with recommended NIST data was made.

The following thermodynamic properties were calculated: compressibility factor, *Z*; enthalpy, *H*; enthalpy of vaporisation, $\Delta^v H$; entropy, *S*; heat capacity at constant pressure, C_P; heat capacity at constant volume, C_V; heat capacity ratio, C_P/C_V; speed of sound, *Ws*; fugacity coefficient, φ; Joule-Thomson coefficient, *JT*. The comparisons with recommended NIST data for these properties were also presented.

The GEOS3C equation gives better predictions of vapour pressure and saturated liquid volume than the other equations of state. The saturated vapour volume is well reproduced by all five equations of state. All the cubic equations predict well the enthalpies and the entropies of the saturated phases and also the isobaric heat capacities, the heat capacity ratio and speed of sound in the same range. The AAD% given in table 3 for the *JT* coefficient in the saturated liquid range are relatively high, determined by very small values of the NIST *JT* coefficients at temperatures where the function changes the sign. The difference in performance between the EOSs is also less noticeable for all thermodynamic properties in the single phase region excepting *JT* coefficient.

The subject has also been discussed in [17].

Acknowledgements: The work has been funded by the Sectoral Operational Programme Human Resources Development 2007–2013 of the Romanian Ministry of Labour, Family and Social Protection through the Financial Agreement POSDRU/107/1.5/S/76813.

List of symbols

a, b, c, d - parameters in GEOS
AAD- absolute average deviation
B- dimensionless parameter in GEOS, defined by eq. (7)
C_1, C_2 and C_3- parameters in GEOS3C temperature function
C_V, C_P- isochoric and isobaric heat capacities
H- enthalpy
JT- Joule-Thomson coefficient
M- molar mass
P, P^S- pressure, saturation pressure
R- universal gaz constant
S- entropy
T- temperature
V, V^L, V^V- molar volume, liquid volume, vapour volume
*W*s- speed of sound
Y- thermodynamic function (general notation)
Z- compresibility factor

Greeks

α_c - Riedel's criterium (parameter in GEOS)
β - reduced temperature function in GEOS
φ- fugacity coefficient
Ω_a, Ω_b, $\Omega_c \Omega_d$- parameters of GEOS
ω - acentric factor

Subscripts

c- critical property
r- reduced property

References

1. ESLAMI H., N. MEHDIPOURB N., BOUSHEHRIB A., International Journal of Refrigeration, 29 (1), 2006, p. 150.
2. MADANIA H., VALTZ A., COQUELET C., MENIAIA A. H., RICHON D., Fluid Phase Equilibria, 268, 2008, p. 68.
3. CHEN Q., HONG R., CHEN G., Fluid Phase Equilibria, 269, 2008, p. 113.
4. JU M., YUN Y., SHIN M. S., KIM H., J. Chem. Thermodynamics, 41, 2009, p. 1339.
5. GEANĂ D., V. FEROIU V., Fluid Phase Equilibria, 174, 2000, p. 51.
6. FEROIU V., GEANĂ D., Fluid Phase Equilibria, 207, 2003, p. 283.
7. FEROIU V., GEANĂ D., SECUIANU C., Rev. Chim. (Bucharest), **59,** 2008, p. 554.
8. NIST - Thermophysical Properties of Fluid Systems, Database 2010, http://webbook.nist.gov/chemistry/fluid/.
9. SOAVE G., Chem. Eng. Sci., 27, 1972, p. 1197.
10. PENG D. Y., ROBINSON D. B., Ind. Eng. Chem. Fundam., 15, 1976, p. 59.
11. SCHMIDT G., WENZEL H., Chem. Eng. Sci., 35, 1980, p. 1503.
12. SALIM P. H., TREBBLE M. A., Fluid Phase Equilibria, 65, 1991, p. 59.
13. GEANĂ D., FEROIU V., Proceedings of the National Conference on Chemistry and Chemical Engineering, Bucharest, Romania, oct. 1995, vol. 3, p. 133.
14. POLISHUK I., Fluid Phase Equilibria, 298, 2010, p. 67.
15. REID R., PRAUSNITZ J.M., POLING B., The Properties of Gases and Liquids, McGraw-Hill, New York, 1986.
16. GEANĂ D., RUS L., Proceeding of the Romanian International Conference on Chemistry and Chemical Engineering (RICCCE XIV), Bucharest, Romania, oct. 2005, vol. 2, p. 170; www.chfiz.pub.ro/laboratories/trl/myweb/termod
17. NOUR, N., DUNA, D., IONITA, M., FEROIU, V., GEANA, D., Rev. Chim. (Bucharest), **64**, no. 10, 2013, p. 1055

Manuscript received: 18.01.2013